Origin of Stick-Slip Motion in Boundary Lubrication

PETER A. THOMPSON AND MARK O. ROBBINS

Molecular dynamics simulations of atomically thin, fluid films confined between two solid plates are described. For a broad range of parameters, a generic stick-slip motion is observed, consistent with the results of recent boundary lubrication experiments. Static plates induce crystalline order in the film. Stick-slip motion involves periodic shear-melting transitions and recrystallization of the film. Uniform motion occurs at high velocities where the film no longer has time to order. These results indicate that the origin of stick-slip motion is thermodynamic instability of the sliding state, rather than a dynamic instability as usually assumed.

ONE OF THE GENERIC PHENOMENA observed when solids slide over each other is stick-slip motion. Instead of moving smoothly, the solids alternately stick together and slip past each other. This oscillatory motion produces most of the squeaks heard in our daily lives and can persist even in the presence of lubricants (*1*).

The usual explanation of stick-slip motion (*1*) is based on the well-known observation that the frictional force *F* on static objects is larger than that on sliding objects. Then, if *F* is a single-valued function of velocity v, it must decrease at small v. In the regime where $dF/dv < 0$, uniform motion is dynamically unstable because decreasing the force increases the velocity. The velocity will oscillate between 0 and a value where $dF/dv > 0$. Measurements have been made for a number of systems (*1, 2*), but it is difficult to confirm the existence of a region where $F(v)$ decreases because of the inherent instability. Another difficulty has been obtaining well-characterized, reproducible, experimental systems.

The latter difficulty has been overcome in recent measurements on atomically flat mica plates separated by fluid films only a few molecules thick (*3–5*). This is a prototypical example of boundary lubrication, an important topic in tribology (*1*). Very precise measurements of stick-slip motion and its dependence on velocity, load, and fluid character have been made (*4, 5*). These results have motivated new theoretical efforts toward understanding the microscopic origin of stick-slip behavior.

We describe here molecular dynamics simulations of boundary lubrication, which reproduce many features of experiments (*1–5*). Analysis of structure in the films reveals that stick-slip motion is associated with periodic phase transitions between ordered static and disordered kinetic states. Temporal or spatial averaging of the force produces decreasing $F(v)$ curves like those assumed in the dynamic instability model of stick-slip motion. However, this confuses cause and effect. The frictional force in the sliding state is a monotonically increasing function of v. The real origin of stick-slip motion is thermodynamic instability of the sliding state below a critical force (and corresponding velocity) rather than a dynamic instability due to $dF/dv < 0$.

To model the experimental system, we considered two solids separated by a thin film of fluid molecules of mass m interacting with a Lennard-Jones (LJ) potential:

$$V(r) = 4\epsilon[(\sigma/r)^{12} - (\sigma/r)^{6}]$$

where ϵ, σ, and $\tau \equiv \sqrt{m\sigma^2/\epsilon}$ are characteristic energy, length, and time scales for the interaction. An LJ potential with modified parameters ϵ_{wf} and σ_{wf} was also used to model interactions between the fluid molecules and discrete wall atoms. The details of this model have been presented in an earlier paper (*6*) in which we examined the influence of ϵ_{wf} and wall geometry on the structure and flow of fluids sheared between solids separated by a distance $h \sim 12\sigma$. For a wide range of parameters, we found that one or more layers of fluid molecules crystallized at the solid surface. This tendency to form a solid wetting phase increased with the degree of corrugation in the wall-fluid potential and with the degree to which the natural spacing of fluid molecules matched that of the wall. For most of the simulations described below, walls were face-centered cubic (fcc) solids with (111) surfaces and density equal to that of the fluid. This face most closely resembles the effective closed-packed structure of mica surfaces (*7*).

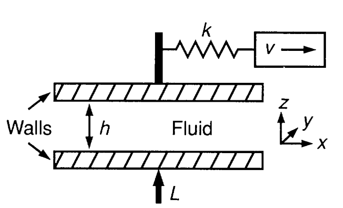

Fig. 1. Sketch of the simulation geometry. Solid walls are held together by a constant normal load *L*. The top wall is pulled by a spring connected to a stage moving at constant velocity v. Periodic boundary conditions are imposed in the *x* and *y* directions.

The wall separation is typically much smaller than 12σ in boundary lubrication. Proximity to two walls amplifies the tendency to order, and the crystallized regions may span the film. For instance, at values of ϵ_{wf} for which a single solid layer formed on each plate at large *h*, we find full crystallization at $h \sim 4\sigma$. Similar results have been observed in experiments (*3–5, 8*) and earlier Monte Carlo studies (*9*).

To mimic boundary lubrication experiments, we performed simulations in a constant load ensemble where *h* was allowed to vary (*10*). A constant temperature $k_bT = 1.1\epsilon$ (k_b is the Boltzmann constant) was maintained by coupling to a heat bath (*6*). At this *T* and nominal density $\rho = 0.81\sigma^{-3}$, the bulk phase is a slightly

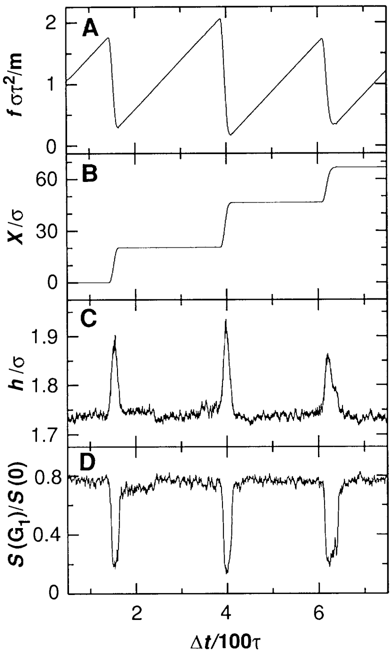

Fig. 2. Time profiles of (**A**) the force per unit area *f*, (**B**) the wall displacement *X*, (**C**) the wall spacing *h*, and (**D**) the Debye Waller factor, during stick-slip motion for a system with $v = 0.1$ $\sigma\tau^{-1}$, $k = 7.2$ $m\tau^{-2}$, $\epsilon_{wf}/\epsilon = 2$, and $\sigma_{wf}/\sigma = 1$. The simulation contains 288 wall and 144 fluid atoms. The walls are fcc solids with (111) surfaces, and the shear direction is (100).

Department of Physics and Astronomy, The Johns Hopkins University, Baltimore, MD 21218.

compressed liquid about 30% above its melting temperature.

As in experiments, the top plate was coupled through a spring with force constant k to a stage moving at constant velocity v (Fig. 1). Initially, the force per unit area applied by the spring, $f \equiv F/A$, is zero and the top plate is at rest. As the stage moves forward, the spring stretches and f increases. If the film is a liquid, the top plate accelerates until the steady-state f balances the viscous dissipation. If the film has crystallized, stick-slip behavior is observed as illustrated in Fig. 2A. Initially, the film responds elastically. The top plate remains stuck, and f increases linearly. Eventually f exceeds the yield stress of the film f_s, and the top plate begins to slide. Since the frictional force is less in the sliding state, the plate accelerates to catch up with the stage and f decreases. At some lower value f_m, the top plate sticks once more, and the process repeats. During the sliding phase, the plate jumps forward by an amount $\Delta x \sim (f_s - f_m)A/k$, approximately 20 to 30$\sigma$ for the case illustrated in Fig. 2B. These forward jumps are typically much larger (~1 μm) in experiments (*3–5*) because weaker spring constants are used (*11*).

Figure 2C shows the plate separation h as a function of time. Since shearing the film increases the effective repulsion between fluid molecules, sliding plates separate at constant normal load. For the stick-slip motion illustrated in Fig. 2, h increases by ~10% during each slip. The resolution of experiments done thus far has not been sufficient to observe changes of this order ($\lesssim 1$ Å), but they had been anticipated on the basis of the "cobblestone" model (*4*).

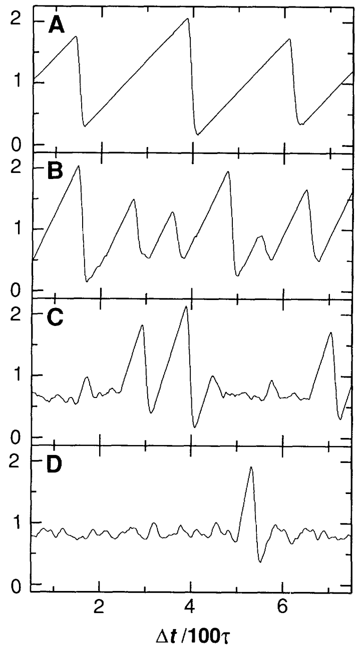

Fig. 3. Time profiles of f at various v for the system of Fig. 2: (**A**) $v = 0.1$, (**B**) $v = 0.2$, (**C**) $v = 0.3$, and (**D**) $v = 0.5$.

The relaxation behavior observed in experiments indicates that substantial rearrangement of the molecules occurs (*5*). We have quantified the time dependence of order in the film by computing the two-dimensional (2-D) structure factor $S(\mathbf{q})$ of the molecules in layers adjacent to the walls. The periodic wall potential induces δ-function peaks in S at wave vectors $\mathbf{q}$ equal to the 2-D reciprocal lattice vectors $\mathbf{G}_i$. In crystallized films, $S(\mathbf{G}_1)/S(0) = e^{-W} \sim 1$, where e^{-W} is the Debye-Waller factor for the shortest reciprocal lattice vector $\mathbf{G}_1$. Figure 2D shows that e^{-W} is close to 1 in the static state, indicating a good solid. However, in the sliding state, $S(\mathbf{G}_1)/S(0)$ drops below 0.2, a value consistent with liquid structure and dynamics (*6, 12*). Snapshots of instantaneous configurations of atoms also show this loss of order.

These observations clearly indicate that the film undergoes solid-liquid phase transitions as it goes from static to sliding states. Analogous transitions termed shear-melting transitions occur when bulk solids are sheared (*13*). Recent theory (*14*) and experiment (*15*) indicate that the ratio of melting stress to shear modulus f_{melt}/c_{44} is ~0.03 to 0.06, depending on the potential and crystal orientation. For low-temperature LJ crystals at the density used in our simulations, $c_{44} \sim 61\ m/\sigma\tau^2$. Thus, the expected $f_{\mathrm{melt}} \sim 1.8$ to $3.6\ m/\sigma\tau^2$ is consistent with the observed yield stress $f_s \sim 2.1\ m/\sigma\tau^2$.

If we interpret stick-slip motion in terms of a first-order shear-melting transition, it is natural to identify spinodal points corresponding to the forces f_u and f_ℓ, where the solid and fluid phases, respectively, are no longer even metastable. One expects these to correspond to f_s and f_m in the appropriate limits. To determine f_ℓ, we performed our simulations with constant force applied to the top plate. Starting from a sliding state, we slowly decreased f until the plates stuck together. For the system shown in Fig. 2, sliding ceased for $f < f_\ell = 0.82\ m/\sigma\tau^2$ ($\overline{v_\ell} \simeq 0.46\ \sigma\tau^{-1}$). Recrystallization should initiate at f_ℓ, but the observed repinning force f_m is lower. The difference depends on the amount of damping. In an underdamped system $f_m < f_\ell$ because f decreases rapidly past f_ℓ at a shear rate that is still large. Experimental systems are usually overdamped. In this case, f decreases slowly and $f_m \sim f_\ell$.

The velocity dependence of the stick-slip behavior is illustrated in Figs. 3 and 4. Figure 3 shows simulation results at four velocities, and Fig. 4 shows the generic F versus v relation. In general, we find a unique yield stress f_s in the limit of small v. However, for a system with (111) solid surfaces, two values corresponding to fcc and hexagonal close-packed ordered phases of the film are observed (Fig. 3A). As v increases, the maximum value of f_s remains fixed, but variations in f_s increase substantially. Intermittent periods without stick-slip motion become more frequent (Fig. 3, B, C, and D). These changes occur because the film does not have enough time to fully order during each stick. Consequently, the mean yield stress decreases as indicated by the squares in Fig. 4. Similar results are found in experiments (*5*). Examination of $S(\mathbf{q})$ shows a direct correlation between the amount of disorder in the film and the observed decrease in f_s. Above a critical velocity v_c, the film remains in a liquid state and slides smoothly.

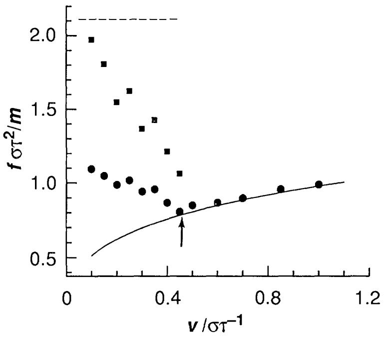

Fig. 4. Force versus v for the system described in Fig. 2. The dashed line and squares denote the maximum and mean yield stress during stick-slip motion, respectively. Circles denote the time-averaged force $\bar f$. The solid line indicates constant-velocity results. The arrow indicates the point (f_ℓ,v_ℓ) at which constant f simulations crystallize.

An experiment without sufficient time resolution would average the stick-slip behavior. Similar averaging occurs in a large system where different regions of the surface may stick and slip at different times. The circles in Fig. 4 indicate the time-averaged $\bar f(v)$ from our simulations. As v increases from 0, there is a linear decrease of $\bar f$ due to increasing disorder in the stuck state and the corresponding decrease in f_s. Above v_c, $\bar f$ increases monotonically.

This curve (Fig. 4) is strikingly similar to the results of earlier measurements (*1*), which did not resolve stick-slip motion. Interpreting it as an intrinsic $F(v)$ curve, one would conclude that stick-slip motion should occur for $v < v_c$ because of the negative slope. However, this confuses cause and effect. Constant v simulations show that $F(v)$ is monotonically increasing in the disordered kinetic state (Fig. 4). The decrease in $\bar F$ results from decreases in the yield stress due to increasing disorder.

We have shown results and presented

discussion for a single geometry. The behavior reported here is quite universal in boundary lubrication by simple fluids. We have also studied different values of ϵ_{wf}, σ_{wf}, and normal load; different crystal faces and shear directions; solid walls with much higher density than the fluid; amorphous walls generated by the rapid quenching of a fluid state; and even the effect of introducing vacancies in the film. In each case, similar stick-slip behavior occurs. What changes are the values of f_s, f_m, and v_c, and the plate separation h_c at which stick-slip behavior starts. For example, we find that increasing the degree of corrugation in the wall-fluid potential increases f_m, v_c, and h_c.

When the walls are amorphous, the order induced in the fluid is no longer crystalline. Instead, a glassy structure that minimizes the wall-fluid interaction is observed. This leads to larger fluctuations in f_s, but the qualitative behavior is similar. Glassy states may also be formed by long-chain molecules between ordered plates because the relaxation of these molecules is slow (*8*). The interplay between molecular structure and ordering during stick-slip motion is an important issue for future work.

Another open question is whether stick-slip motion is caused by analogous mechanisms in other systems. The ordered static and disordered sliding states need not correspond to solid and fluid structure in an intermediate film. Instead, in the case of solid-on-solid sliding, they may correspond to states with and without chemical bonds or elastic deformations that increase the coupling between plates. For example, stick-slip motion of a weak solid over a hard solid leaves behind patches of the weak material (*1*), suggesting periodic welding of the surfaces followed by cracking. These and other possibilities remain to be explored.

REFERENCES AND NOTES

1. See, for example, F. P. Bowen and D. Tabor, *Friction and Lubrication* (Oxford Univ. Press, Oxford, 1958); E. Rabinowicz, *Friction and Wear of Materials* (Wiley, New York, 1965).
2. C. Scholz, P. Molnar, T. Johnson, *J. Geophys. Res.* 77, 6392 (1972).
3. J. N. Israelachvili, P. M. McGuiggan, A. M. Homola, *Science* **240**, 189 (1988); A. M. Homola, J. N. Israelachvili, M. L. Gee, P. M. McGuiggan, *J. Tribol.* **3**, 675 (1989).
4. P. M. McGuiggan, J. N. Israelachvili, M. L. Gee, A. M. Homola, *Mater. Res. Soc. Symp. Proc.* **140**, 79 (1989).
5. M. L. Gee, P. M. McGuiggan, J. N. Israelachvili, A. M. Homola, *J. Chem. Phys.* **93**, 1895 (1990).
6. P. A. Thompson and M. O. Robbins, *Phys. Rev. A* **41**, 6830 (1990).
7. R. Erlandsson, G. Hadziioannou, C. Mate, G. McClelland, S. Chiang, *J. Chem. Phys.* **89**, 5190 (1988).
8. J. Van Alsten and S. Granick, *Phys. Rev. Lett.* **61**, 2570 (1988); *Langmuir* **6**, 876 (1990); *Tribol. Trans.* **33**, 436 (1990).
9. M. Schoen, C. L. Rhykerd, Jr., D. J. Diestler, J. H. Cushman, *Science* **245**, 1223 (1989).
10. The simulations were performed in a constant number, load, and temperature ensemble. The number of fluid molecules N is not fixed in experiments. However, the time scale of stick-slip events is too short to allow significant transport from the bulk.
11. In the limit of infinitely stiff springs, the forward jump may reduce to a single lattice constant as seen in simulations of solid-on-solid sliding by U. Landman, W. D. Luedtke, and A. Nitzan [*Surf Sci.* **210**, L177 (1990)].
12. In particular, the shear plane in bulk films is very close ($<\sigma$) to the solid wall for $e^{-W} \sim 0.2$ (*6*).
13. B. J. Ackerson and N. A. Clark, *Phys. Rev. Lett.* **44**, 1005 (1980); *ibid* **46**, 123 (1981).
14. M. J. Stevens, M. O. Robbins, J. F. Belak, in preparation.
15. P. M. Chaikin, J. M. diMeglio, W. D. Dozier, H. M. Lindsay, D. A. Weitz, in *Physics of Complex and Supermolecular Fluids*, S. Safran and N. A. Clark, Eds. (Wiley-Interscience, New York, 1987), pp. 65–81.
16. We thank J. N. Israelachvili, P. M. McGuiggan, and M. J. Stevens for useful conversations. Supported through NSF grant DMR 85-53271 and allocations at the Pittsburgh Supercomputing Center. The work of M.O.R. was supported by the Sloan Foundation and through NSF grant PHY 82-17853 at the Institute for Theoretical Physics, where this project was conceived. The work of P.A.T. was supported by the Johns Hopkins University Applied Physics Laboratory.

8 May 1990; accepted 10 August 1990

Pressure Dependence of Elastic Wave Velocity for β-Mg_2SiO_4 and the Composition of the Earth's Mantle

GABRIEL D. GWANMESIA, SALLY RIGDEN, IAN JACKSON,
ROBERT C. LIEBERMANN

The pressure dependence of the elastic wave velocities for hot-pressed, elastically isotropic polycrystals of the β (modified spinel) phase of magnesium orthosilicate (Mg_2SiO_4) has been determined at room temperature to 3 gigapascals (GPa) by ultrasonic pulse interferometry. Pressure derivatives of the bulk ($dK/dP = 4.8$) and shear ($dG/dP = 1.7$) moduli derived from the travel times of the compressional (P) and shear (S) waves clearly demonstrate that the velocity contrast between the olivine and β phases of Mg_2SiO_4 decreases with increasing pressure. When combined with plausible values for the (as yet unmeasured) temperature derivatives, these new data can be used to calculate the contrast in P and S wave velocities across an olivine–β phase transformation occurring at pressure-temperature conditions corresponding to about 400 kilometers depth in the earth. The seismologically observed contrasts ΔV in both P and S wave velocities constrain the percentage of orthosilicate in a model mantle of uniform chemical composition for appropriate relative magnitudes of the temperature (T) derivatives of the bulk and shear moduli for the β phase. Allowed combinations of orthosilicate content (percent), dK/dT, and dG/dT (both in gigapascals per Kelvin) for a pair of recent seismological models with $\Delta V_P = \Delta V_S = 4.6\%$ include (65, −0.018, −0.020), (55, −0.015, −0.018), and (45, −0.012, −0.016).

A CONTINUING CHALLENGE FOR Earth scientists has been to determine the relative contributions of isochemical phase transformation and chemical stratification to the discontinuous increases of seismic wave velocity with depth that characterize the transition zone (400 to 670 km depth) of the earth's mantle. A detailed knowledge of the chemical composition of the earth's mantle is vital in placing constraints on the early formation of the earth and on its thermal and chemical evolution.

Pioneering studies (*1*) suggested that phase transformations might play an important role in explaining the velocity and density structure of the transition zone. Subsequently it was demonstrated that the dominant minerals of the upper mantle (olivine and pyroxene) transform to more close-packed crystal structures under the pressure-temperature conditions of the transition zone (*2*) and that these transformations are likely to produce relatively sharp seismic discontinuities (*3*). In particular, the discontinuous increase in seismic wave velocity near 400 km depth has been attributed at least in part to the transformation of $(Mg,Fe)_2SiO_4$ olivine to the β phase (*4*).

More quantitative assessment of the nature of the 400-km discontinuity has been facilitated by measurements under ambient conditions of the elastic properties of single-crystal β-Mg_2SiO_4; these studies revealed that there is a ~13% contrast in elastic wave velocities between the olivine and β phases (*5, 6*). However, the conclusions of recent

---

G. D. Gwanmesia and R. C. Liebermann, Mineral Physics Institute and Department of Earth and Space Sciences, State University of New York at Stony Brook, Stony Brook, NY 11794.
S. Rigden and I. Jackson, Research School of Earth Sciences, Australian National University, Canberra, A.C.T., 2601, Australia.